J Mater Sci (2006) 41:6425–6430
DOI 10.1007/s10853-006-0715-2

Preparation of high dispersed nickel pastes for thick film electrodes

D. H. Im · S. H. Hyun · S. Y. Park · B. Y. Lee · Y. H. Kim

Received: 5 March 2004 / Accepted: 22 June 2005 / Published online: 12 August 2006

Abstract Ultra-thinning of Ni paste films for BME-MLCC (Base Metal Electrode Multilayered Ceramic Capacitor) internal electrode was investigated. Adding various dispersants, ball-milling powder, and using the pre-dispersion process to improve Ni paste dispersion and properties of the paste electrodes/thick films, were employed. The paste containing 200 nm sized Ni powders, ethyl cellulose vehicle ($\eta = 2.98 \times 10^4$ mPa-s at 0.1 s^{-1}), and Emphos PS-21A as a dispersant proved to be the most desirable candidate. This paste thick film showed the smallest surface roughness ($R_a = 0.10$ μm and $R_{max} = 0.97$ μm) at a viscosity ($\eta = 2.80 \times 10^5$ mPa-s at 0.1 s^{-1}) adaptable to screen-printing. In addition, the Ni paste/thick film had the low sheet resistivity ($\rho = 1.11 \times 10^{-4}$ Ωcm) and an excellent microstructure after sintering at 1,290 °C for 3 h in a 97% N_2/3% H_2 atmosphere.

Introduction

Metal pastes are currently used commercially for the production of various electrical and electronic components such as solar cells, multilayer ceramic capacitors (MLCC), multichip modules, and hybrids. All these applications require finely structured conductive layers, which are usually produced with screen-printing technologies, using metal powders containing print pastes. In the miniaturization of electronic devices like MLCC, using metal pastes as electrodes has rapidly advanced. This trend to embrace MLCC is based on the need for cost effective electronic devices with a compact chip configuration that are small in size, yet high in volumetric efficiency and reliability [1].

The capacitance of MLCC can be enhanced through not only developing dielectric and electrode layers of less than 5 μm thickness but also increasing the number of layers. However, creating these thinner dielectric and internal electrode layers are problematic. There tends to be breakage of the electrodes, and structural defects of the MLCCs, which contribute to the short circuiting between electrode layers, when the primary particles are not refined and are not homogeneously dispersed in paste without agglomeration.

In recent years, MLCCs containing the internal electrodes made from Ni pastes instead of Pt/Pd pastes have been successfully developed to satisfy a variety of needs of high performance capacitors at a low cost [2, 3]. To prepare for the rising demands, it is necessary to make nano sized Ni powders with a narrow range of size distribution to improve the dispersibility of Ni within the paste. The synthesizing methods to make nano scaled Ni powders have already been investigated [4–6], while the research about the dispersion of Ni powders during the processing of Ni paste is relatively lacking. Under specified conditions, our group has previously examined the effect of various dispersants in Ni pastes and the electrode properties of Ni paste thick films for MLCC internal electrodes using 500 nm sized Ni powders.

D. H. Im · S. H. Hyun (✉) · S. Y. Park
School of Advanced Materials Science and Engineering, College of Engineering, Yonsei University, 134, Sinchon-dong, Seodaemun-gu, Seoul 120-749, Korea
e-mail: prohsh@yonsei.ac.kr

B. Y. Lee · Y. H. Kim
Changsung R&D Center, Changsung Corporation, Namdong Industrial Area 11-9, Namdong-gu, Incheon 405-100, Korea

This article reports on our evaluation of effective dispersants and the degree of the paste dispersion used in fabricating Ni pastes. In addition, the effect of the pre-dispersion process, the vehicle viscosity on the paste dispersion before screen-printing and the dispersion and surface roughness of Ni powder after screen-printing were investigated.

Experimental

The overall experimental flow chart for this study on fabricating Ni paste is given in Fig. 1, and the detailed experimental procedure in each step is stated below.

Ni powders were obtained from Changsung Co. Ltd, Korea. The specific surface area and particle size distribution of these powders were measured by the BET surface area analyzer (ASAP 2010, Micromeritics, USA) and particle size analyzer (PSA, PAR-III, Otsuka Electronics Co., Osaka, Japan), respectively.

The thick film pastes for MLCC internal electrode were formulated having the composition of nickel powders as the functional material, ceramic paste ($BaTiO_3$ powders: vehicle = 40:60) as the sintering suppressor, a mixture of ethyl cellulose (EC, HE 350, HE 10, Japan), and Terpineol (Fluka, Swiss) as a vehicle, and a dispersant; the ratio of the composition was kept at 47.5:30:19.5:3, respectively. Dispersants used for this investigation were TEA (Triethanolamine, Duksan, Korea), $(PEO\text{-}PCL)_b$ (Poly(ethylene oxide)-block-polycaprolactone, 4-arm) (Aldrich, USA), ethylene glycol (Junsei, Japan), Emphos PS-21A (Witco, USA), and Y-company's dispersant (Japan). If the dispersant was a powder type like $(PEO\text{-}PCL)_b$, the dispersant was dissolved in Terpineol and used. The pastes were prepared and homogenized on a 3-roller mill (EXAKT 35, Germany) after premixing and aging at 50 °C for 10 min. The thick film patterns of area 2 cm × 5 cm, were screen-printed onto a glass slide substrate using a stainless steel 250 mesh screen. The screen-printed films were dried at 100 °C for 10 min and then the surface roughness of the dried thick film was measured. The other thick film patterns with an area of 0.7 cm × 1.1 cm were screen-printed onto $BaTiO_3$ (X7R) green sheet with an area of 1.1 cm × 1.3 cm using the same 250 mesh for observing microstructure after sintering. The pastes sintered in an industrial thick-film firing furnace at 1,290 °C for 3 h in a 97% N_2/3% H_2 atmosphere after burning out at 270 °C for 26 h in an air atmosphere.

The microstructure of the nickel powder, screen-printed pastes, and the resultant fired films were observed with a scanning electron microscope (SEM, Model S4200, Hitachi, Tokyo, Japan). Rheological behavior of the pastes was determined using a cone/plate rheometer (HA-DV III$^+$, Brookfield, USA), and the surface roughness of the dried thick film was measured using the contact surface roughness profilometer (SE3500, Kosaka Laboratory Ltd., Japan). The surface roughness of the dried thick films was presented by the average value of 5 times per 2.5 mm on the film surface. The sheet resistance of the fired films was measured using the four-point technique.

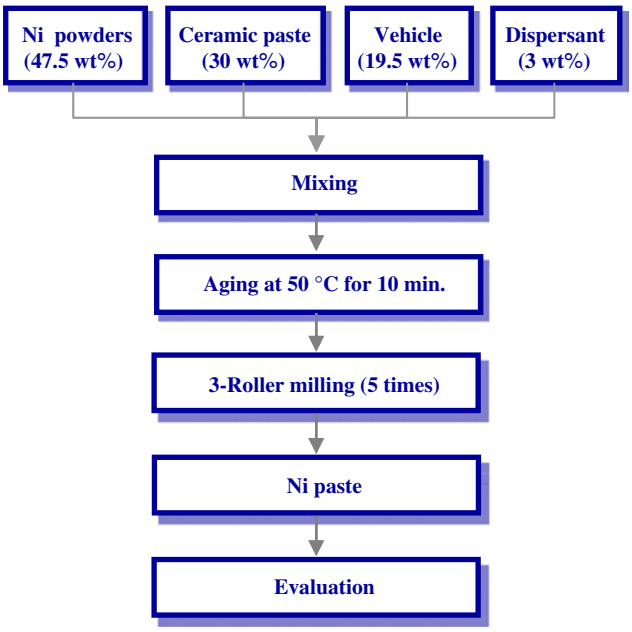

Fig. 1 Overall experimental flow chart

Results and discussion

Powder characteristics

The SEM micrographs and particle size distribution of Ni powders as a functional material are shown in Fig. 2. The primary particle size and specific surface area of these powders were 200 nm from Fig. 2a and 4.33 m^2/g, respectively. But some agglomerates existed in the region of above 1 μm from Fig. 2b. This agglomeration of Ni primary particles occurs as particle size decreases because of a quantum size effect and a magnetic force.

Dispersion properties of pastes

The dispersion of paste was influenced by various factors such as the size and surface property of powders, interaction between powders and vehicle, the viscosity of the vehicle and final paste, 3-roller milling processing, and additives like dispersant.

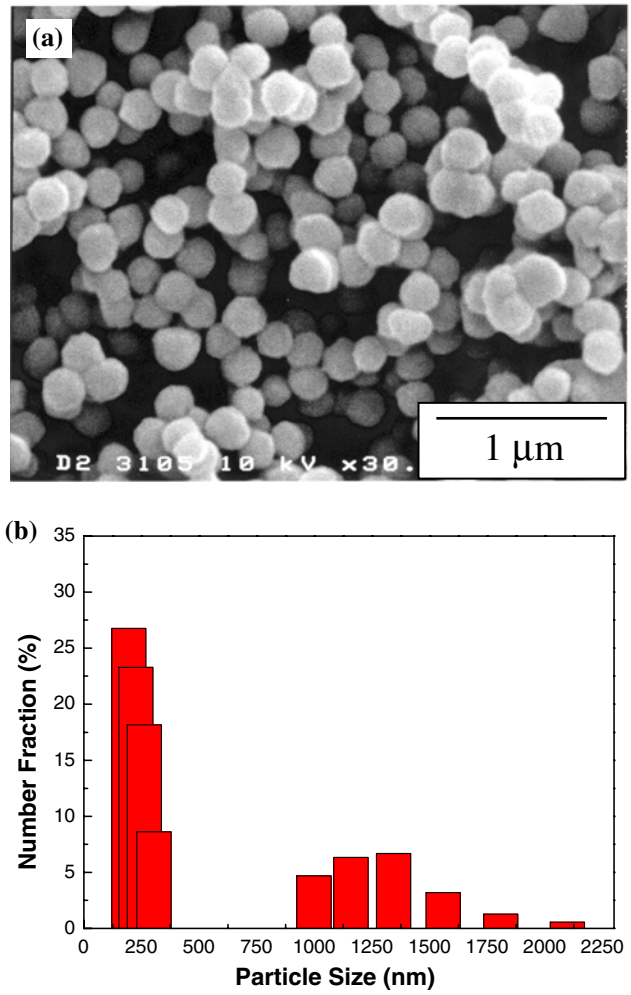

Fig. 2 SEM micrograph and particle size distribution of nickel powders in this work

Among those factors, the effect of dispersant has been examined in our previous report [7]. Using the same method, Table 1 shows the surface roughness of Ni pastes depending on dispersants. When using Emphos PS-21A, the paste showed the smallest R_a and R_{max}.

Patton [8] reported that the flow properties generated by paint components separate into the two shear rate regions. The viscosity, in the ultra-low shear rate range below 0.1 s^{-1}, is dominated by the minor rheological additives, particle flocculation or binder dispersion. In this study, the dispersants were chosen after observing the viscosity variations in the shear range of 0.01~0.1 s^{-1}. The effect of these dispersants on viscosity variations of Ni pastes is shown in Fig. 3. The viscosity variations of Ni pastes containing Emphos PS-21A and ethylene glycol showed relatively low values from 0.01 s^{-1} to 0.1 s^{-1}. Although the viscosity curve did not show complete pseudoplastic flow for Emphos PS-21A, it was chosen from the roughness and viscosity results as an effective dispersant because it created an uniform surface for screen-printing Ni paste.

Table 1 Surface roughness of Ni pastes depending on dispersants

Dispersant	Surface roughness (μm)	
	R_a	R_{max}
No dispersant	0.17	3.08
Y-company dispersant	0.23	3.88
$(PEO\text{-}PCL)_b$ + Terpineol	0.18	3.76
TEA	0.16	3.22
Ethylene glycol	0.16	3.11
Emphos PS-21A	0.14	1.90

Figure 4 shows the effect of powder pulverization on Ni paste. Ueyama et al. [2] reported that Ni paste containing highly mono dispersed Ni powders after pulverization improved the surface roughness. But metal powders such as Ni and Cu can deform by extra mechanical shock and stress due to their ductility and malleability. In order to determine optimum ball-milling time, which satisfied both the high removal rate of agglomerates and little deformation of powders, the removal rate of agglomerates according to increasing ball-milling time was observed. Fig. 4 shows that agglomerates of Ni powders decreased significantly up until 8 h and then remained relatively unchanged with increased ball-milling times. Consequently, the paste that consisted of Ni powders after ball-milling, with the maximum surface roughness (R_{max} = 1.17 μm) of Ni paste noticeably decreased compared to the value (R_{max} = 1.90 μm) before ball-milling.

The pre-dispersion process was attempted to obtain the homogeneous mixed state of the components and uniform surface of paste after screen-printing. The pre-dispersion process in this study was defined as having only Ni powders and vehicle mixing on a 3-roller mill three times, and then the ceramic paste

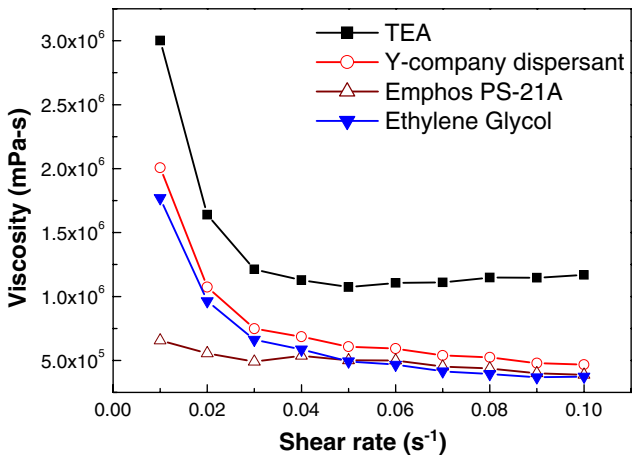

Fig. 3 Effect of dispersants on the viscosity variations of Ni pastes at 22 °C

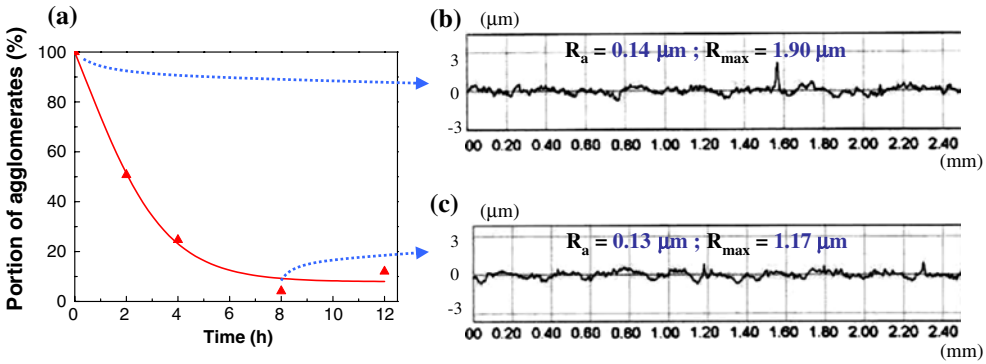

Fig. 4 (**a**) Agglomerate portion of Ni powders in EtOH versus ball-milling time and surface roughness variations of Ni paste (**b**) before and (**c**) after ball-milling

was added to the mixture of Ni powders and vehicle and milled two times on a residuary 3-roller mill.

Figure 5 shows the schematic diagram of pre-dispersion processing and the surface roughness of Ni pastes. Although R_a and R_{max} of the paste fabricated by pre-dispersion process reduce the value by 10% compared to that made by the one step dispersion process, the weak point of the pre-dispersion process is that the paste processing increases by two steps thus decreasing the operation efficiency.

In general, the viscosity of paste using small powders is higher than that of large powders. These phenomena can be explained by the following equation:

$$V_{\text{eff}} = V(1 + \delta/\alpha)^3$$

where V_{eff} is the effective volume fraction of solids which determine the viscosity of slurry, δ is the thickness of the polymer layer, α is the radius of spherical particle and V is the volume fraction of the solids. If the dispersant forms a monolayer of polymer on the particles, the smaller the particles are, the higher the effective volume is. That means although the net solid content is the same, the smaller powder needs more solvent to be wet and holds more space than the coarser powder. So the smaller powder has a higher viscosity [9]. Therefore, to obtain simultaneously the optimum viscosity and uniform surface of the paste, we controlled the paste viscosity by decreasing the viscosity of the vehicle as a dispersion media.

Figure 6 shows rheological behavior of 9 wt% solutions of different types of ECs and mixed ECs in 66% terpineol/25% mineral oil. As the shear rate increase, the solution exhibits a shear thinning behavior. A high viscosity vehicle indicated the solution of a high molecular EC (mixture of HE 350 and HE 10), while a low viscosity vehicle resulted in a low molecular weight EC (HE 10). When the mixing ratio of vehicle mixture is 3:1 (HVV:LVV), the viscosity of the vehicle was about half the value (2.98×10^4 mPa-s at 0.1 s^{-1}).

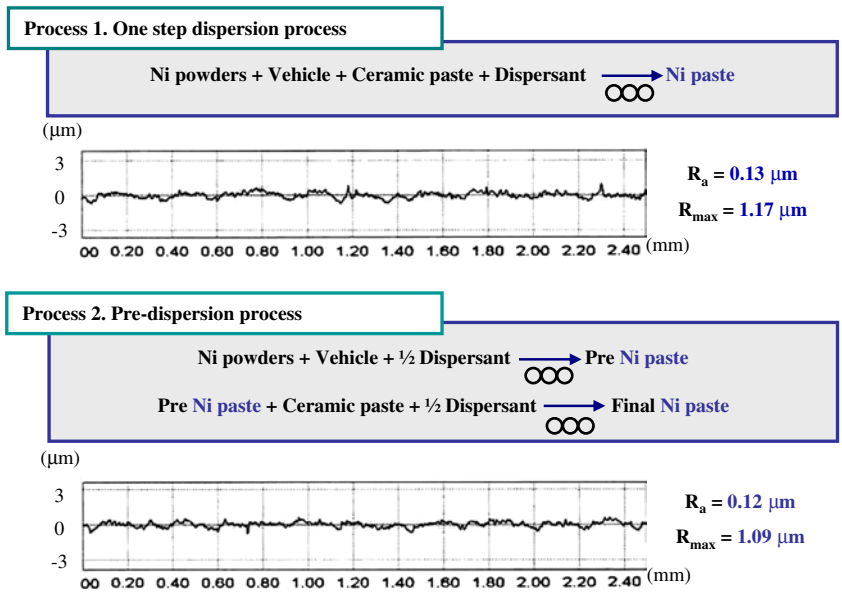

Fig. 5 Dispersion processes and surface roughness variations of Ni paste

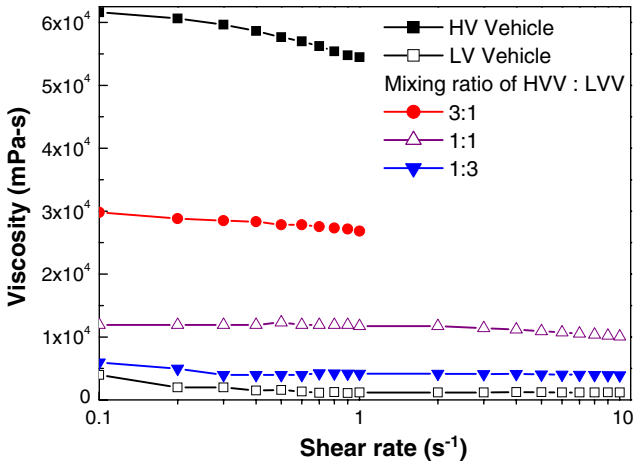

Fig. 6 Viscosity variations according to ethyl cellulose type and mixing ratio

The viscosity variations of Ni paste using the mixing vehicle whose ratio is 3:1 (HVV:LVV) are shown in Fig. 7. The curve shows the desirable shear-thinning tendency when the viscosity of the paste is 2.80×10^5 mPa-s at the shear rate of 0.1 s^{-1}, that is, it is an adaptable viscosity for screen-printing [7]. Moreover, the surface roughness of Ni paste was enhanced as the value of R_a = 0.10 μm and R_{max} = 0.97 μm. The above results can be explained that the viscosity of the vehicle is strongly related to screen-printability and dispersion. The particles were easily leveling because of the interaction between powders and the optimum vehicle viscosity.

Microstructure and resistivity of thick films

The SEM micrographs of the dried thick films of the Ni paste that consisted of 200 nm sized Ni powder are shown in Fig. 8a and b. These morphologies show simply the mixing form of Ni powders (200 nm) and $BaTiO_3$ powders (100 nm). As shown in Fig. 8, the morphology of fracture surface demonstrated mostly uniformity and a few peaks of agglomerate in one part. This appearance is also seen in the value of surface roughness.

Figure 9 shows the SEM micrographs of the Ni thick films after sintering. Enormous sintered grains of the Ni powders and of the $BaTiO_3$ powders were observed. Lin and Wang [10] also expressed that the dispersion degree, which has an effect on the morphology and densification of the thick film after burning out, of inorganic particles in the vehicle is a deciding factor in making the capillary force homogeneous in the drying and the burning out processes. And the density of fired films is intimately associated with the dispersion of inorganics in the vehicle. This occurs because the vehicle in this homogeneous dispersion gets evaporated during drying, yielding a smooth dried print due to uniform shrinkage.

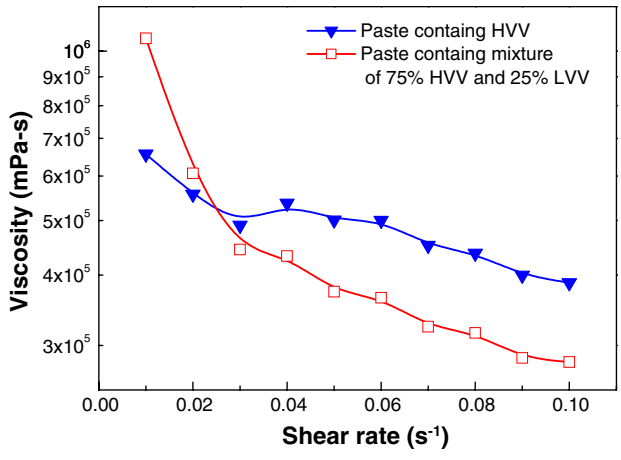

Fig. 7 Effect of mixed vehicle on viscosity variations of Ni paste at 22 °C

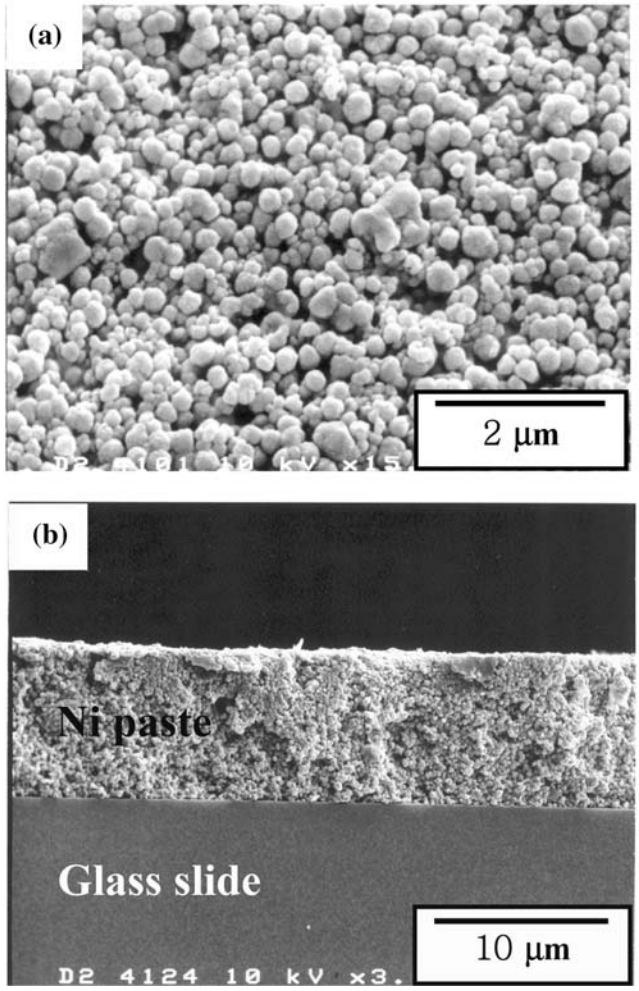

Fig. 8 SEM micrographs of Ni pastes after drying at 100 °C for 10 min: (**a**) surface and (**b**) cross section of films

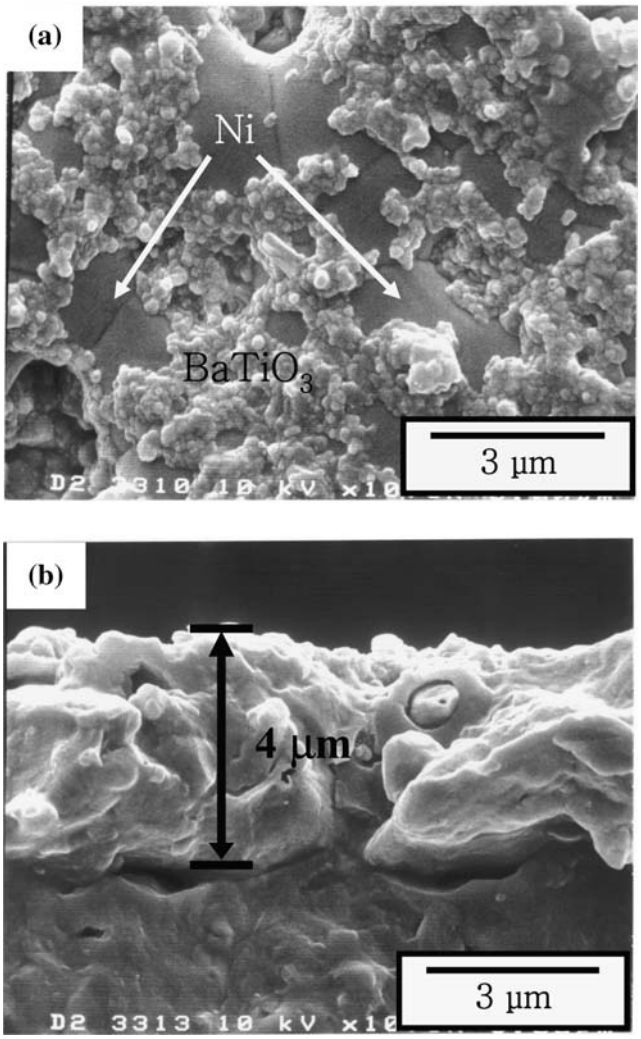

Fig. 9 SEM micrographs of Ni thick films after sintering at 1,290 °C for 3 h in 97% N_2/3% H_2 atmosphere: (**a**) surface and (**b**) cross section of films

There are no defects within the many large grains, in the fired thick film, proving good sintering properties can be achieved by using fine powders and homogeneous mixing. As a result, the sheet resistivity of the thick film was 1.11×10^{-4} Ωcm. The resistivity of standard bulk Ni is 7×10^{-6} Ωcm, indicates that the resistivity of the obtained film is quite high. This is because the $BaTiO_3$ powders, which were added to paste as a shrinkage suppressor for reducing the difference in thermal expansion coefficients between Ni electrode and dielectric layers, play a role as an insulator within the conducting Ni electrodes.

Conclusions

The properties of Ni paste electrode/thick film as an internal electrode of MLCC were demonstrated. Through adding various dispersants, ball-milling powder, and using the pre-dispersion process, we attempted to obtain the homogeneous mixed state of the components and the uniform surface of paste after screen-printing. First of all, it is shown that the Emphos PS-21A as a dispersant, which reduced surface roughness and viscosity, was highly effective in improving the powder dispersion in paste. In addition, the ball-milling of Ni powders for 8 h effectively reduced the maximum surface roughness of Ni paste and the pre-dispersion process improved the surface roughness of Ni paste by a value of 10%.

Using vehicle viscosity control, the Ni paste containing 200 nm sized Ni powders, Emphos PS-21A as a dispersant, and a mixture of 75% HVV and 25% LVV had the smallest surface roughness (R_a = 0.10 μm and R_{max} = 0.97 μm) and an adaptable viscosity ($\eta = 2.80 \times 10^5$ mPa-s at 0.1 s^{-1}) for screen-printing.

The dispersion degree of Ni paste intimately related to thick film properties after sintering. The Ni thick film made from Ni paste with the uniform surface and acceptable viscosity had low sheet resistivity ($\rho = 1.11 \times 10^{-4}$ Ωcm) and uniformly large grain microstructure.

Acknowledgement The authors would like to acknowledge the financial assistance of the Ministry of Information and Communication of Korea supported by the IMT-2000 project.

References

1. Ueyama R, Ueyama T, Koumoto K, Kuribayashi K (2001) J Ceram Soc Jpn 109(8):661
2. Ueyama R, Seki N, Kamada K, Harada M, Ueyama T (1999) J Ceram Soc Jpn 107(7):652
3. Yamamatsu J, Kawano N, Arashi T, Sato A, Nakano Y, Nomura T (1996) J Power Sources 60:199
4. Zheng H, Liang J, Zeng J, Qian Y (2001) Mater Res Bull 36:947
5. Gao J, Guan F, Zhao Y, Yang W, Ma Y, Lu X, Hou J, Kang J (2001) Mater Chem Phys 71:215
6. Chou KS, Huang KC (2001) J Nanoparticle Res 3:127
7. Im DH, Hyun SH, Park SY, Lee BY, Kim YH *Mater. Sci. Eng. A* (under review)
8. Patton TC (1968) J Paint Technol 40(522):301
9. Sun J, Gao L, Guo J (1998) J Nanostruct Mater 10(6):1081
10. Lin JC, Wang CY (1996) Mater Chem Phys 45:253